CHEMICAL ENGINEERING TRANSACTIONS
VOL. 60, 2017
A publication of AIDIC
The Italian Association of Chemical Engineering
Online at www.aidic.it/cet
Guest Editors: Luca Di Palma, Elisabetta Petrucci, Marco Stoller

ISBN978-88-95608- 50-1; **ISSN** 2283-9216
DOI: 10.3303/CET1760026

Complete Removal of Persistent Pesticide Using Reduced Graphene Oxide−Silver Nanocomposite

Maria Sarno, Marcello Casa*, Claudia Cirillo, Paolo Ciambelli

Department of Industrial Engineering and Centre NANO_MATES University of Salerno, Via Giovanni Paolo II ,132 - 84084 Fisciano (SA), Italy
mcasa@unisa.it

Reduced graphene oxide supporting silver nanoparticles, obtained by an efficient, “green” and one step “top-down” solution route, was used for removal from water of chlordane, a known persistent organic pollutants. A two-step mechanism, involving chlordane degradation by Ag nanoparticles and subsequent adsorption of the degraded products: ether bis(2-chloro allyl), 1,10-dichlorodecane and octadecanoid acid were detected, on the reduced graphene oxide surface, leads to a complete removal of chlordane from water solution in only 11 minutes at room temperature.

1. Introduction

The increasing use of noxious compounds led to devastating effect not only for the environment but also for human health (Kutz et al. 1992). Among various organic and inorganic pollutants, chlorinated pesticides have significant toxicity to plants or animals, including humans; in particular chlordane (1,2,4,5,6,7,8,8-octachloro-3a,4,7,7a-tetrahydro-4,7-methanoindane) is a known persistent organic pollutants (POP), classified among the "dirty dozen" and banned by the 2001 Stockholm Convention on Persistent Organic Pollutants. In the years 1948–1988 chlordane was a common pesticide for corn and citrus crops, it adheres to soil particles and enters groundwater, requiring many years to degrade. Chlordane is very resistant to chemical and biological degradation. Once in water bodies, it is not removed by photodegradation, hydrolysis or biodegradation and has a high bioaccumulation potential. In the last decades, however, with reference to composite materials, molecular adsorption and reaction on graphene and graphene based composites and their applications in water purification (Sreeprasad et al. 2011; Sreeprasad et al. 2013) have gained great momentum. Indeed, special properties, such as large surface area (Zhu et al. 2010) antibacterial nature (S. Liu et al. 2011b), reduced cytotoxicity (Chang et al. 2011), and tunable chemical properties (Tuček et al. 2014) make these materials very attractive choices for this application. Metal/graphene nanocomposites are very effective reducing agent for dehalogenation and can contemporaneously reduce catalytically various halogenated organics into low- or non- toxic compounds, followed by successive adsorption of the degraded products by the graphene surface (Sarno et al. 2016a). In particular, silver decorated graphene nanocomposite, due to the high specific surface area of graphene and the well-known catalytic properties of silver in oxidation reactions (Wiley-VCH 2011), have been demonstrated to be promising catalyst for numerous applications, such as: aerobic oxidation of benzyl alcohol (Zahed and Hosseini-Monfared 2015); dye catalysts for wastewater treatment (Jiao et al. 2015, Casa et al. 2016); but also hydrogenation of phenols (Liu et al. 2017). In this paper, we report on the chemical reactivity of reduced graphene oxide decorated with silver nanoparticles (rGO_Ag) in degrading halogenated pesticides, taking chlordane as case study. rGO_Ag have been obtained by a novel one-step “top-down” synthetic strategy, providing experimental easiness, potential low-cost fabrication and negligible environmental impact. Homogeneously dispersed nanoparticles (NPs) on completely exfoliated rGO were prepared, able to degrade chlordane in a very short time also if compared with previously results (Sarno et al. 2016a). We have found that chlordane removal involves a two-step mechanism: degradation of chlordane by Ag nanoparticles and subsequent adsorption of the degraded products by the rGO surface.

Please cite this article as: Sarno M., Casa M., Cirillo C., Ciambelli P., 2017, Complete removal of persistent pesticide using reduced graphene oxide−silver nanocomposite, Chemical Engineering Transactions, 60, 151-156 DOI: 10.3303/CET1760026

2. Experimental Section

2.1 Materials

Graphite powder (synthetic, 99.9 %, SIGMA ALDRICH), sulphuric acid (H_2SO_4, 95-97 %, SIGMA ALDRICH), potassium permanganate ($KMnO_4$, ≥ 99 %, SIGMA ALDRICH), hydrogen peroxide (H_2O_2, 30 %, SIGMA ALDRICH), L-ascorbic acid (vitamin C, ≥ 99 %, SIGMA ALDRICH), $AgNO_3$: silver nitrate, ≥ 99.9 %, SIGMA ALDRICH, sodium hydroxide (NaOH, ≥ 98 %, pellets, SIGMA ALDRICH), ethanol (reaction grade, ≥ 99.8 %, FlukaAnalytical), bi-distilled water (Fluka Analytical) were used as received.
1000 mg/L of chlordane stock solution was prepared by dissolving the required amount of chlordane in pure n-hexane (99.9%) and kept under refrigerated condition.

2.2 Synthesis of rGO_Ag

We synthesized reduced graphene oxide (rGO) starting from GO obtained by a modified Hummers method (Chen et al. 2009). Indeed it has been established that the reduction of graphene oxide provides a shortcut to mass production of graphene. Then, a one-step procedure provides graphene oxide reduction, and the simultaneous nanoparticles precipitation, occurring through silver nitrate reduction favoured by the GO functionalities (a “site selective” precipitation). This is a very easy and fast procedure in which four different water solution batches: of GO (1 g/l); of reducing agent (Vitamin C, 15 g/l); of silver nitrate (5 g/l); and of ammonia(few drops),were mixed together and kept for 2 hour at 98 °C. During silver nanoparticles precipitation, $AgNO_3$ dissolves in water solution forming the Tollens’ reagent with ammonia, that in the presence of a mild reducing agent led to the precipitation of metallic silver.

2.3 Degradation and AdsorptionExperiments

All adsorption studies were done in 20ml batch reactors at room temperature keeping 5 ml of rGO_Ag dispersion (0.01 wt.%) as working volume. A required amount of chlordane stock solution was spiked to the rGO_Ag dispersion to get the working concentration of chlordane at 2 mg/l. The solutions were stirred during 11 min. The liquid was separated from the dispersion using a 200 nm membrane filter paper.
The filtrate, extracted with hexane, was analysed for residual chlordane and its degradation products using gas chromatography (GC) (ThermoFisher). The analysis conditions were set as follows: run time, 16.5 min; injector temperature, 200 °C; 80°C for 1min+from 80°C to 185°C 10°C/min+185°C for 5 min, 1 ml/min.

2.4 Characterization

Transmission electron microscopy (TEM) images were acquired using a FEI Tecnai electron microscope operated at 200 KV with a LaB_6 filament as the source of electrons, equipped with an EDX probe.
Raman spectra were obtained at room temperature with a micro-Raman spectrometer RenishawinVia with a 514 nm excitation wavelength (laser power 30 mW) in the range 100-3000 cm^{-1}. XRD measurements were performed with a Bruker D8 X-ray diffractometer using CuKα radiation. Thermogravimetric analysis (TG-DTG) at 10 K/min heating rate in flowing air was performed with a SDTQ 600 Analyzer (TA Instruments) coupled with a mass spectrometer.

3. Results and discussion

3.1 rGO_Ag Characterization

Figure 1 shows the XRD pattern of rGO_Ag. The spectra shows the typical peaks of silver nanoparticles at about 2θ = 38°, 45°, 65°, 78° and 82°, corresponding to (1 1 1), (2 0 0), (2 2 0), (311) and (2 2 2) planes, respectively (JCPDS File No.: 01-1167), with the majority of particles showing (1 1 1) plane having face-centered cubic (fcc) structure (Xu and Hu 2012). The particles size has been evaluated by the Scherrer formula (Singh 2005):

$$\tau = \frac{K \cdot \lambda}{(FWHM - b) \cdot \cos\theta}$$

Where K is structural constant (depending on the shape of the particle), λ is the wavelength of X-ray, τ is the mean size of the nanoparticles, FWHM is full width at half maximum of the signal and b is the instrumental broadening. Using this formula, the average particle size is 10 nm ± 1.9 evaluated as mean from the different peaks. The lattice spacing (*a*)of the cubic crystal, namely the distance of the metal atoms in the structure has been evaluated to be 4.126 Å , from the signal position.
Raman spectra of GO, and rGO_Ag, in the wavenumber range 800−2200 cm^{-1}, are shown in Figure 2. The samples show two prominent peaks: the G band at approximately 1590 cm^{-1} due to the first-order scattering

of the E_{2g} phonons, and the D band around 1350 cm^{-1}that is a breathing mode of A_{1g} symmetry involving phonons near the K zone boundary (Sarno et al. 2016b). The intensity of the D band is related to the size of the in-plane sp^2 domains and the relative intensity ratio (I_D/I_G) is a measure of the distance between defects, L_D, that gives an idea of the extent of disorder (Konios et al. 2014). After GO reduction and Ag precipitation, the I_D/I_G intensity ratio increases from 0.81 of GO to 1.1, indicating an increased L_D distance between defect, meaning a good reduction level. In addition, it is worth noticing that the intensities of these bands are enhanced significantly after the decoration of Ag NPs on the surface of rGO. This is due to the Ag NPs deposited on rGO which enhance the Raman signal via the Surface-Enhanced Raman Spectroscopy (SERS) effect (Nafiey et al. 2016).

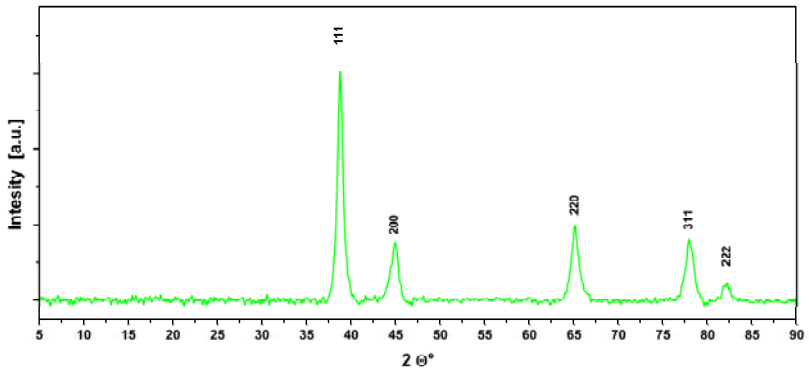

Figure 1. X-ray diffraction pattern of rGO_Ag

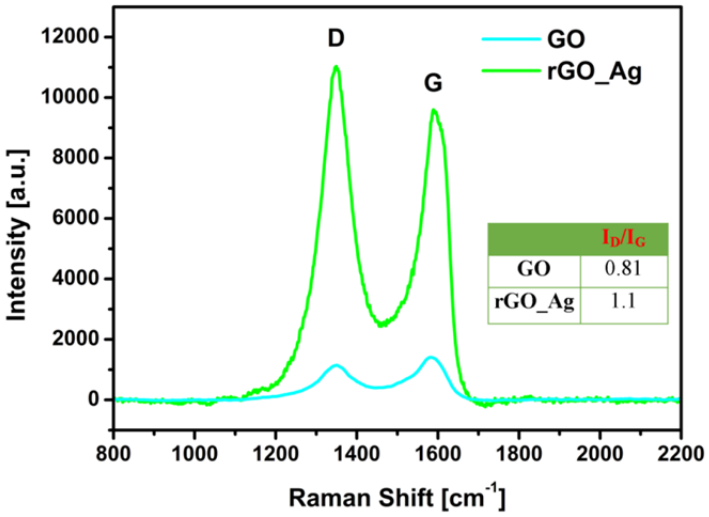

Figure 2. Raman Spectrum of rGO_Ag and GO

Figure 3 shows a bright-field TEM image of silver coated graphene. It demonstrates that monodispersed silver nanoparticles dispersed uniformly on graphene surface can be obtained by the one step synthetic approach. It is worth noticing that silver nanoparticles are present only on the graphene surface also after the sonication procedure used to prepare sample for TEM images.

Thermogravimetric analysis was used to evaluate the thermal stability and Ag loading for rGO_Ag. The TGA (TG-DTG) profile is shown in Figure 4. After a weight loss due to water in the range between 25 and 100 °C, a weight loss due to reduced graphene oxide decomposition/oxidation takes place in different steps, probably due to the morphology of the sample. At first, the decomposition of the external planes of graphene takes place, then, around 300°C the inner carbon of the graphene skeletal are oxidised. Unlike the graphitic species, the carbon lattice oxidation starts at lower temperature (200°C instead of 400-600°C), likely due to a silver nanoparticles catalytic effect on oxidation reactions (Kim and Ryu 2011). Moreover, the residues at 1000°C are due to silver nanoparticles.

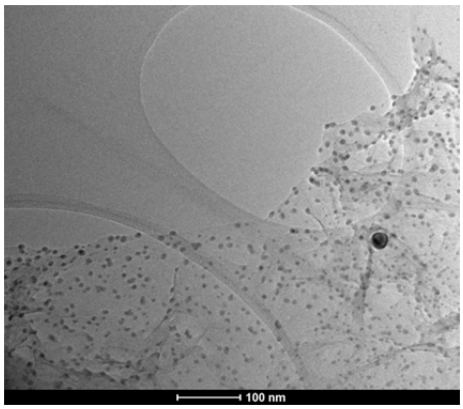

Figure 3. rGO_AgTEM image

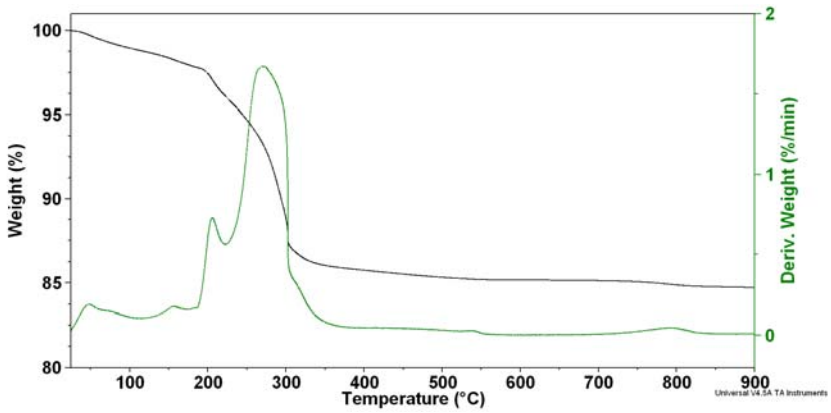

Figure 4. TG-DTG profiles of rGO_Ag

3.2 Degradation and adsorption tests

Chlordane, from the stock solution, was spiked in a rGO_Ag water dispersion (2 mg/l final chlordane concentration) to test the composite reactivity. GC analysis was carried out to monitor the chlordane concentration evolution(see the GC-MS spectrum of chlordane in Figure 5). Before test, the chlordane solution presented a peak around a retention time of 8 minutes together with a solvent peak (hexane) during the first two minutes, in the GC spectrum.

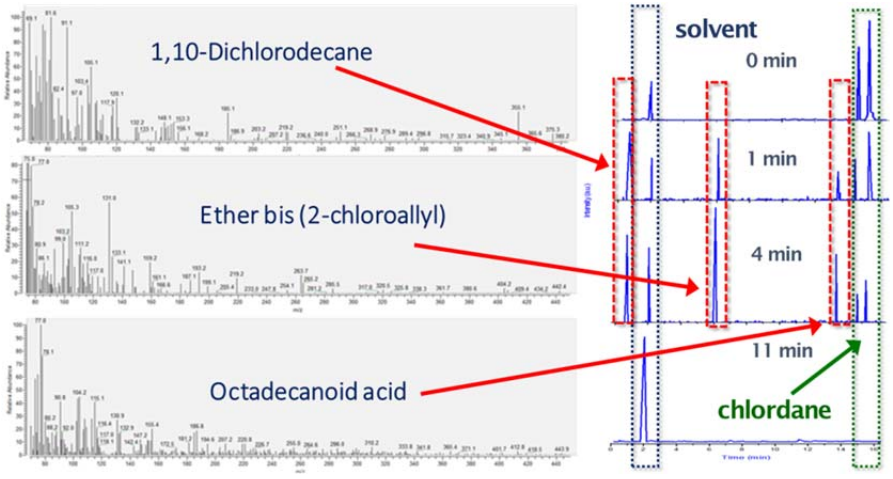

Figure 5. GC-MS spectrum of chlordane (a) and after test (b.

With increasing the reaction time the chlordane peaks started to disappear, implying its removal from the solution, new peaks, coming from degradation products (Ether bis(2-chloroallyl), 1,10-dichlorodecane and octadecanoid acid), became more and more visible at retention time slower than chlordane. Moreover, when the solution was stirred for 11 min (see Figure 5), the peaks of both chlordane and reaction products disappeared, it is probably due to the combined degradation and π-π (Gupta et al. 2015, Liu et al. 2011) adsorption between the hydrocarbons unsaturation and rGO π orbitals. Thus, chlordane was completely removed quickly in 11 min due to the excellent catalytic performance of the silver and absorbing properties of graphene. On the other hand, further analysis at closer times and investigations will be carried out in order to better understand the reaction and absorption roles in the removal of the pesticide (surface absorption analysis, e.g. XPS, EDX, ..).

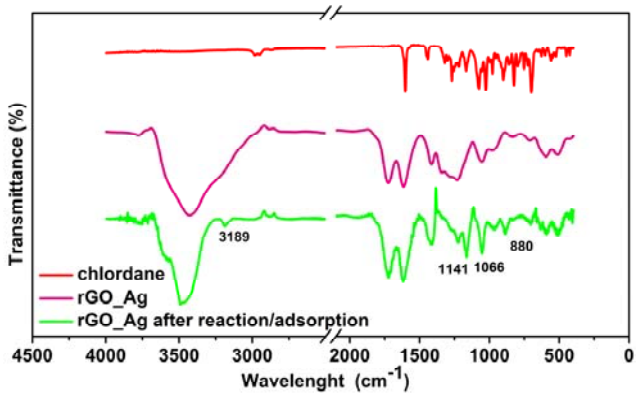

Figure 6. IR spectra of chlordane (red), rGO_Ag (violet line), rGO_Ag after reaction/adsorption (green line)

In the IR spectrum of rGO_Ag after reaction/adsorption (Figure 6, green line) new peaks at about 880, 1066 and 1141 cm^{-1} , respect to the rGO_Ag as produced (violet line), due to the bending vibrations of the =C-H group and a weak peak at 3189 cm^{-1} due to aromatic C-H stretching occurs, giving an indication of the formation of aromatic products adsorbed on nanocomposites surface. After the reaction with chlordane, rGO_Ag, well dispersed in water during the tests due to its hydrophilic nature, can be easily separated under the action of a magnetic field.

4. Conclusion

TEM image of rGO_Ag shows that the nanoparticles have diameter of 10 nm and they are homogeneously dispersed on graphene surface. Furthermore, a sustainable and efficient way for dehalogenation of halocarbon using rGO_Ag was presented. This process removes completely in only 11 min a persistent organochlorine pesticide. The catalyst/adsorber is very efficient and may be employed for the degradation of other toxic halocarbons.

References

Casa M., Sarno M.,Cirillo C., Ciambelli P., 2016, Reduced Graphene Oxide-Based Silver Nanoparticle Containing Natural Hydrogel as Highly Efficient Catalysts for Nitrile Wastewater Treatment, Chemical Engineering Transactions, 47, 307-312.

Chang Y., Yang S.-T., Liu J.-H., Dong E., Wang Y., Cao A., Liu Y., Wang H., 2011, In Vitro Toxicity Evaluation of Graphene Oxide on A549 Cells, Toxicology Letters, 200, 201–210.

Chen T., Zeng B., Liu J. L., Dong J. H., Liu X. Q., Wu Z., Yang X. Z., Li Z. M., 2009, High Throughput Exfoliation of Graphene Oxide from Expanded Graphite with Assistance of Strong Oxidant in Modified Hummers Method, Journal of Physics: Conference Series, 188, 12051.

Gupta S. S., Chakraborty I., Maliyekkal S. M., Mark T. A., Pandey D. K., Das S. K., Pradeep T., 2015 Simultaneous Dehalogenation and Removal of Persistent Halocarbon Pesticides from Water Using Graphene Nanocomposites: A Case Study of Lindane, ACS Sustainable Chemistry and Engineering, 3, 1155–1163.

Jiao T., Guo H., Zhang Q., Peng Q., Tang Y., Yan X., Li B., 2015, Reduced Graphene Oxide-Based Silver Nanoparticle-Containing Composite Hydrogel as Highly Efficient Dye Catalysts for Wastewater Treatment, Scientific Reports, 5, 11873.

Kim S. C., Ryu J. Y., 2011, Properties and Performance of Silver-Based Catalysts on the Catalytic Oxidation of Toluene, Environmental Technology, 32, 561–568.

Konios D., Stylianakis M., Stratakis E., Kymakis E., 2014, Dispersion Behavior of Graphene Oxide and Reduced Graphene Oxide, Journal of Colloid and Interface Science, 430, 108–112.

Kutz F. W., Cook B. T., Carter-Pokras O. D., Brody D., Murphy R. S., 1992, Selected Pesticide Residues and Metabolites in Urine from a Survey of the U.S. General Population, Journal of Toxicology and Environmental Health, 37, 277–291.

Liu F.; Chung S.; Oh G.; Seo T. S., 2011a, Three-dimensional graphene oxide nanostructure for fast and efficient water-soluble dye remova,l ACS Applied Materials and Interfaces, 4, 922– 927

Liu S., Zeng T. H., Hofmann M, Burcombe E., Wei J., Jiang R., Kong J., Chen Y., 2011b, Antibacterial Activity of Graphite, Graphite Oxide, Graphene Oxide, and Reduced Graphene Oxide: Membrane and Oxidative Stress, *ACS Nano,* 5, 6971–6980.

Liu J., Ran C., Pu Y., Wang J. -X., Wang D., Chen J. –F., 2017, Silver/graphene Nanocomposites as Catalysts for the Reduction of P-Nitrophenol to P-Aminophenol: Materials Preparation and Reaction Kinetics Studies, The Canadian Journal of Chemical Engineering.

Nafiey A. Al, Subramanian P., Addad A., Sieber B.,Szunerits S., Boukherroub R., 2016, Green Synthesis of Reduced Graphene Oxide-Silver Nanoparticles Using Environmentally Friendly L-Arginine for H_2O_2 Detection, ECS Journal of Solid State Science and Technology, 5, M3060–M3066.

Sarno M., Cirillo C., Ciambelli P., 2016a, Dehalogenation and Contemporaneous Removal of Halocarbon using Graphene/Ni Nanoparticles, Chemical Engineering Transactions, 47, 169-174.

Sarno M., Baldino L., Scudieri C., Cardea S., Ciambelli P., Reverchon E., 2016b, Supercritical CO_2 Processing to Improve the Electrochemical Properties of Graphene Oxide, The Journal of Supercritical Fluids, 118, 119–12.

Singh A. K., 2005, Advanced X-Ray Techniques in Research and Industry, Hyderabad, India: IOS Press.

Sreeprasad T.S., Gupta S. S., Maliyekkal S. M., Pradeep T., 2013, Immobilized Graphene-Based Composite from Asphalt: Facile Synthesis and Application in Water Purification, Journal of Hazardous Materials, 246–247, 213–220.

Sreeprasad T.S., Maliyekkal S. M., Lisha K. P., Pradeep T., 2011, Reduced Graphene Oxide–metal/metal Oxide Composites: Facile Synthesis and Application in Water Purification, Journal of Hazardous Materials,186, 921–931.

Tuček J., Kemp K. C., Kim K. S., Zbořil R., 2014, Iron-Oxide-Supported Nanocarbon in Lithium-Ion Batteries, Medical, Catalytic, and Environmental Applications, ACS Nano, 8, 7571–7612.

Wiley-VCH, 2011, Ullmann's Encyclopedia of Industrial Chemistry, 40 Volume *Set*. 7 edition. Weinheim, Wiley-VCH.

Xu Z., Hu G., 2012, Simple and Green Synthesis of Monodisperse Silver Nanoparticles and Surface-Enhanced Raman Scattering Activity, RSC Advances, 2, 11404–11409.

Zahed B., Hosseini-Monfared H, 2015, A Comparative Study of Silver-Graphene Oxide Nanocomposites as a Recyclable Catalyst for the Aerobic Oxidation of Benzyl Alcohol: Support Effect, Applied Surface Science 328, 536–547.

Zhu Y., Murali S., Cai W., Li X., Suk J. W., Potts J. R., Ruoff R. S., 2010,Graphene and Graphene Oxide: Synthesis, Properties, and Applications, Advanced Materials, 22, 3906–3924.